# Thermodynamic Functions of Molecular Conformations of (2-Fluoro-2-phenyl-1-ethyl)ammonium Ion and (2-Hydroxy-2-phenyl-1-ethyl)ammonium Ion as Models for Protonated Noradrenaline and Adrenaline: First-Principles Computational Study of Conformations and Thermodynamic Functions for the Noradrenaline and Adrenaline Models

**DongJin R. Lee,[†] Natalie J. Galant,[†] Hui Wang,[‡,§] Zoltan Mucsi,[†] David H. Setiadi,[†,||] Bela Viskolcz,*[,§] and Imre G. Csizmadia[†,§,||,⊥]**

*Department of Chemistry, University of Toronto, Toronto, Ontario, Canada M5S 3H6, College of Chemistry, Beijing Normal University, Xin Wai Street 19, Hai Dian, Beijing, 100875, China, Department of Chemical Informatics, Faculty of Education, University of Szeged, Boldogasszony sgt. 6, Szeged H-6725, Hungary, Global Institute of Computational Molecular and Materials Science, and Drug Discovery Research Center*

*Received: August 17, 2008; Revised Manuscript Received: January 7, 2009*

This paper reports the structural and thermodynamic consequences of substitution of the OH group by the isoelectronic F-atom in the case of the adrenaline family of molecules. The conformational landscapes were explored for the two enantiomeric forms of N-protonated-$\beta$-fluoro-$\beta$-phenyl-ethylamine, also called (2-fluoro-2-phenyl-1-ethyl)-ammonium ion (Model 1) and that of N-protonated-$\beta$-hydroxy-$\beta$-phenyl-ethylamine, also referred to as (2-hydroxy-2-phenyl-1-ethyl)-ammonium (Model 2) models of noradrenaline and adrenaline molecules. These full conformational studies were carried out by first principles of quantum mechanical computations at the B3LYP/6-31G(d,p) and G3MP2B3 levels of theory, using the Gaussian03 program. Also, frequency calculations of the stable structures were performed at the B3LYP/6-31G(d,p), and G3MP2B3 levels of theory. The thermodynamic functions (U, H, S, and G) of the various stable conformations of the title compounds were calculated at these levels of theory for the R and S stereoisomers. Relative values of the thermodynamic functions have been calculated with respect of the chosen reference conformers in which all relevant dihedral angles assumed anti orientation for the Model 1 and Model 2. Through the combination of both point and axis chirality, the enantiomeric and diastereomeric relationships of the six structures for each molecule investigated were established. Intramolecular hydrogen bonding interactions have been studied by the atoms in molecules (AIM) analysis of the electron density. The aromaticity of phenyl group has been determined by a selective hydrogenation protocol. The pattern of the extent of aromacity, due intramolecular interactions, varies very little between the two models studied.

## 1. Introduction

**1.1. Historical Background.** As reviewed[1] in 1900, in May 1886, William Bates reported in the *New York Medical Journal* the discovery of a substance produced by the adrenal gland.[1] Less than a decade later, in 1895, the Polish physiologist Napoleon Cybulski also isolated this substance and identified it as adrenaline (Figure 1). Within the next 5 years, independent discoveries of adrenaline were made by John Jacob Abel and Jokichi Takamine as well.[2,3] Within 4 years, it was synthesized for the first time by the German chemist Friedrich Stolz;[4] adrenaline was the first hormone to be crystallized.[4]

**1.2. Biological Background.** Adrenaline is a member of the catecholamine family[5] and, as a biogenic amine, acts as both hormone and neurotransmitter.[6,7] Primarily, adrenaline is known to be synthesized in the adrenal medulla. The known major effects of adrenaline include increased heart rate and stroke volume, pupil dilation, and arteriole constriction.[8] Adrenaline also elevates plasma glucose levels by directly enhancing glycogen breakdown and, furthermore, inhibits insulin and stimulates glucagon secretion.[9−11]

Adrenaline moderates nerve pulses to efferent organs. Consequently, the catecholamine family and its analogs, such as adrenaline, are widely studied.[12] The release of adrenaline from the adrenal medulla is one of the first responses to stressors and fear, and thus, adrenaline is capable of regulating cardiovascular function during dynamic exercise.[13]

Recent computational and experimental studies of adrenaline have indicated that the conformation of catecholamine neurotransmitters autoregulate receptor binding and thus directly control the rate of metabolism.[14] Therefore, it is necessary to study the energetically stable and accessible conformation of adrenaline in order to fully understand the hormone's function. The majority of conformational studies, conducted to date, have been performed in the gas phase or in apolar solvents because most receptor sites are known to be strongly hydrophobic. The intramolecular hydrogen bonds are, in fact, favored in these hydrophobic environments. Consequently, contribution of such apolar environment of the receptor site is considerable in controlling the high concentrations of internally hydrogen-bonded adrenaline conformers.[14] Moreover, naturally occurring neurotransmitters containing aryl-ethylamines are found to affect mood. Most mood-changing drugs and antidepressants perform

[†] University of Toronto.
[‡] Beijing Normal University.
[§] University of Szeged.
[||] Global Institute of Computational Molecular and Materials Science; www.giocomms.org.
[⊥] Drug Discovery Research Center; www.drugcent.com.

10.1021/jp807353n CCC: $40.75 
Published on Web 02/24/2009

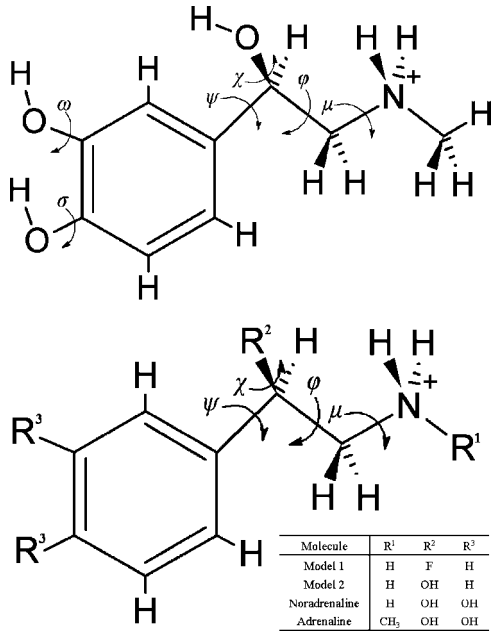


**Figure 1.** (A) Protonated adrenaline and six dihedral angles as conformational variables. (B) Structures of protonated adrenaline, noradrenaline, and two model compounds. Dihedral angles as conformational variables are clearly indicated.

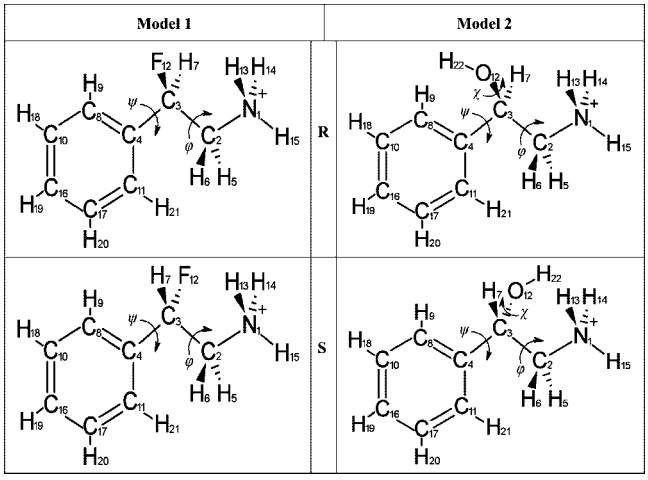


**Figure 2.** Two enantiomers of model 1 N-protonated-$\beta$-fluoro-$\beta$-phenyl-ethylamine and model 2 N-protonated-$\beta$-hydroxy-$\beta$-phenyl-ethylamine.

their functions as enzyme−inhibitors or receptor agonists/antagonists.[15]

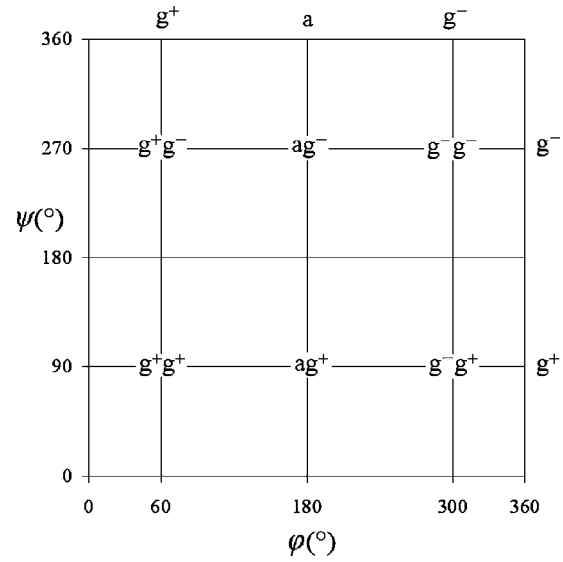


**Figure 4.** Topological pattern of the conformers of model 1, N-protonated-$\beta$-fluoro-$\beta$-phenyl-ethylamine, enantiomers to be geometry optimized at the B3LYP/6-31G(d,p) and G3MP2B3 levels of theory.

## 2. Scope

The structure of adrenaline, noradrenaline, as well as models 1 and 2 are shown in Figure 2. The purpose of these conformational studies of models 1 and 2 is to determine the preferred conformational structures of noradrenaline and adrenaline model molecules (Figure 2) by ab initio restricted Hartree−Fock (RHF) and density functional theory (DFT) computation. Conformational analysis provides information of energy change as a function of a single or several variables

$$E = f(\phi) \quad \text{potential-energy curve}$$

$$E = f(\psi, \phi) \quad \text{potential-energy surface}$$

The two dihedral angles, $\varphi$ and $\Psi$, are the two principle single bonds about which internal rotation generates distinctly different conformations. This research focused on the variation of $\varphi$ and $\Psi$ torsional angles in order to determine the relative stabilities of the various conformers existing on the potential-energy surface. In general, the $g+$, $a$, and $g-$ conformations are considered to be stable conformers.

The dihedral angles shown in Figure 2 were defined as follows: $\varphi = N_1C_2-C_3C_4$, $\Psi = C_2C_3-C_4C_8$, and $\chi = C_2C_3-O_{12}H_{22}$. To explore the conformational space of the noradrenaline and adrenaline models studied (Figure 2), the variation of the following dihedral angles were studied: $\varphi$ equals gauche+

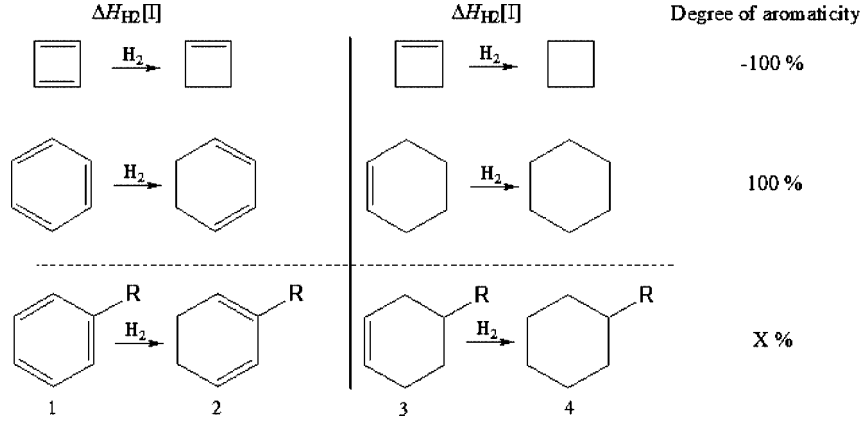


**Figure 3.** Definitions for calculation of the aromaticity percentage.

**TABLE 1: Dihedral Angles Ψ and φ, Total and Relative Energies of Model 1, N-Protonated-β-fluoro-β-phenyl-ethylamine, Computed at the G3MP2B3 and [B3LYP/6-31G(d,p)] Levels of Theory**

| | G3MP2B3 and [B3LYP/6-31G(d,p)] | | | | | | | |
|---|---|---|---|---|---|---|---|---|
| parameters | Ψ (deg) | | φ (deg) | | energy (Hartree) | | Δ*E* (kcal/mol) | |
| *R* [g+ g+] | 81.53 | [82.22] | 54.86 | [54.51] | −465.817117 | [−465.837772] | 3.05 | [3.15] |
| *R* [g− g+] | −95.59 | [−94.98] | 55.01 | [54.61] | −465.817115 | [−465.837772] | 3.05 | [3.15] |
| *R* [g+ a] | 72.26 | [72.4] | −167.66 | [−167.29] | −465.821982 | [−465.842791] | 0.00 | [0.00] |
| *R* [g− a] | −106.77 | [−106.71] | −167.67 | [−167.21] | −465.821982 | [−465.842791] | 0.00 | [0.00] |
| *R* [g+ g−] | 102.42 | [102.23] | −63.37 | [−63.36] | −465.824276 | [−465.845065] | −1.44 | [−1.43] |
| *R* [g− g−] | −75.64 | [−75.72] | −62.96 | [−63.25] | −465.824275 | [−465.845063] | −1.44 | [−1.43] |
| *S* [g++] | 75.62 | [75.81] | 63.08 | [63.34] | −465.824276 | [−465.845064] | −1.44 | [−1.43] |
| *S* [g− g+] | −102.03 | [−101.65] | 63.17 | [63.38] | −465.824279 | [−465.845064] | −1.44 | [−1.43] |
| *S* [g+ a] | 106.82 | [106.92] | 167.67 | [167.21] | −465.821982 | [−465.84279] | 0.00 | [0.00] |
| *S* [g− a] | −72.23 | [−72.3] | 167.64 | [167.17] | −465.821982 | [−465.842791] | 0.00 | [0.00] |
| *S* [g+ g−] | 95.73 | [94.96] | −54.73 | [−54.7] | −465.817118 | [−465.837772] | 3.05 | [3.15] |
| *S* [g− g−] | −81.5 | [−82.21] | −54.59 | [−54.7] | −465.817118 | [−465.837772] | 3.05 | [3.15] |

(60°), anti (180°), and gauche− (−60°), while Ψ could be at syn (0°), anti (180°), gauche+ (90°), and gauche− (−90°).

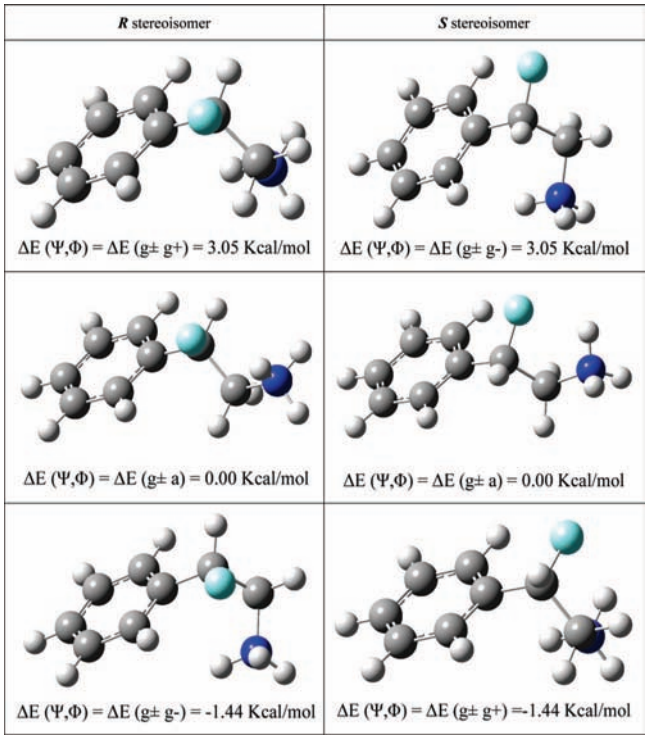


**Figure 5.** All conformations of the *R* and *S* configurations of model 1, N-protonated-β-fluoro-β-phenyl-ethylamine, computed at the G3MP2B3 level of theory with the corresponding relative energy values. (Note that each row has a pair of enantiomers that are equal in energy.)

## 3. Methods

**3.1. Exploratory Computations.** All computations were carried out using the Gaussian 03 program package (G03).[16] Each structure was initially optimized using the ab initio[17] restricted Hartree−Fock (RHF)[18] method using the standard split valence 3-21G basis set that is incorporated in G03.[19−21] Total and relative energies are given in the Supporting Information (Table S1).

**3.2. Detailed Computations.** The RHF/3-21G full geometry-optimized structural parameters of each conformer of N-protonated-β-fluoro-β-phenyl-ethylamine and N-protonated-β-hydroxy-β-phenyl-ethylamine were used as input to calculate relative energies at the B3LYP/6-31G(d,p) level of theory.[22,23] Total energies were computed in hartrees, and the relative energies are given in kilocalories per mole.

**3.3. Advanced Computations.** The G3-based quantum chemistry method (G3MP2B3) was employed to yield even more reliable relative energies of each geometry-optimized conformer at the B3LYP/6-31G(d,p) level of theory. G3MP2B3[24−26] denotes the Gaussian-3-based (G3) Møller−Plesset second-order (MP2) method in combination with the 6-31G(d,p) basis set.

**3.4. Molecular Vibrations.** The frequencies and intensities of each stable conformer of N-protonated-β-fluoro-β-phenyl-ethylamine and N-protonated-β-hydroxy-β-phenyl-ethylamine were calculated at the B3LYP/6-31G(d,p) and G3MP2B3 levels of theory to verify their conformations as being true minima.

**3.5. Thermodynamic Functions (*U*, *H*, *G*, *S*).** The thermodynamic functional changes of thermally corrected energy (Δ*U*), enthalpy (Δ*H*), Gibbs free energy (Δ*G*), and entropy (Δ*S*) were calculated for the optimized conformations. The *U*, *H*, and *G* values were computed in hartrees, and their relative values are

**TABLE 2: Thermodynamic Functional Changes of Energy (Δ*U*), Enthalpy (Δ*H*), Gibbs Free Energy (Δ*G*), and Entropy (Δ*S*) of Model 1, N-Protonated-β-fluoro-β-phenyl-ethylamine, Computed at the B3LYP/6-31G(d,p) and G3MP2B3 Levels of Theory**

| | G3MP2B3 and [B3LYP/6-31G(d,p)] | | | | | | | |
|---|---|---|---|---|---|---|---|---|
| parameters | Δ*U* (kcal/mol) | | Δ*H* (kcal/mol) | | Δ*G* (kcal/mol) | | Δ*S* (cal/mol·K) | |
| *R* [g+ g+] | 3.06 | [3.14] | 3.06 | [3.14] | 3.34 | [3.42] | −0.93 | [−0.94] |
| *R* [g− g+] | 3.06 | [3.14] | 3.06 | [3.14] | 3.35 | [3.41] | −0.95 | [−0.93] |
| *R* [g+ a] | 0.00 | [0.00] | 0.00 | [0.00] | 0.00 | [0.00] | 0.00 | [0.00] |
| *R* [g− a] | 0.00 | [0.00] | 0.00 | [0.00] | 0.00 | [0.00] | 0.01 | [0.01] |
| *R* [g+ g−] | −1.33 | [−1.33] | −1.33 | [−1.33] | −1.19 | [−1.18] | −0.47 | [−0.51] |
| *R* [g− g−] | −1.33 | [−1.33] | −1.33 | [−1.33] | −1.18 | [−1.18] | −0.50 | [−0.49] |
| *S* [g+ g+] | −1.33 | [−1.33] | −1.33 | [−1.33] | −1.19 | [−1.18] | −0.49 | [−0.50] |
| *S* [g− g+] | −1.33 | [−1.33] | −1.33 | [−1.33] | −1.17 | [−1.18] | −0.54 | [−0.49] |
| *S* [g+ a] | 0.00 | [0.00] | 0.00 | [0.00] | 0.00 | [−0.01] | 0.01 | [0.04] |
| *S* [g− a] | 0.00 | [0.00] | 0.00 | [0.00] | 0.00 | [−0.01] | 0.01 | [0.02] |
| *S* [g+ g−] | 3.06 | [3.14] | 3.06 | [3.14] | 3.33 | [3.42] | −0.90 | [−0.94] |
| *S* [g− g−] | 3.06 | [3.14] | 3.06 | [3.14] | 3.32 | [3.42] | −0.89 | [−0.94] |

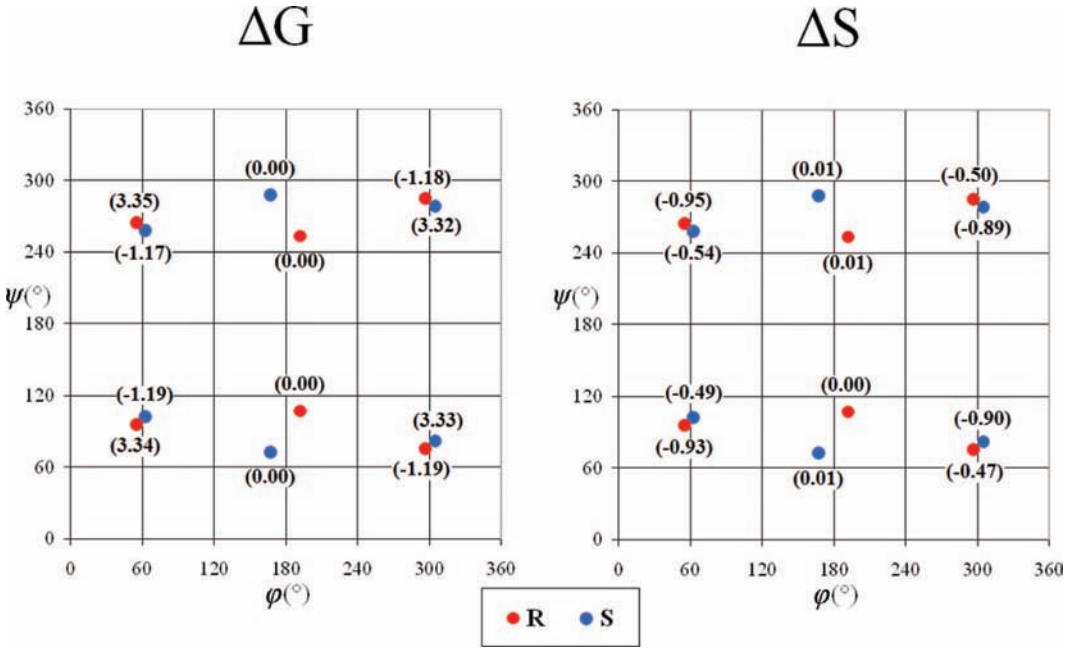


**Figure 6.** Topological representation of the optimized geometries of Model 1, N-protonated-$\beta$-fluoro-$\beta$-phenyl-ethylamine, dihedral angles $\Psi$ and $\varphi$ corresponding to the vertical and horizontal axes, respectively. Relative energies are given in units of kcal/mol and calculated at the G3MP2B3 level of theory.

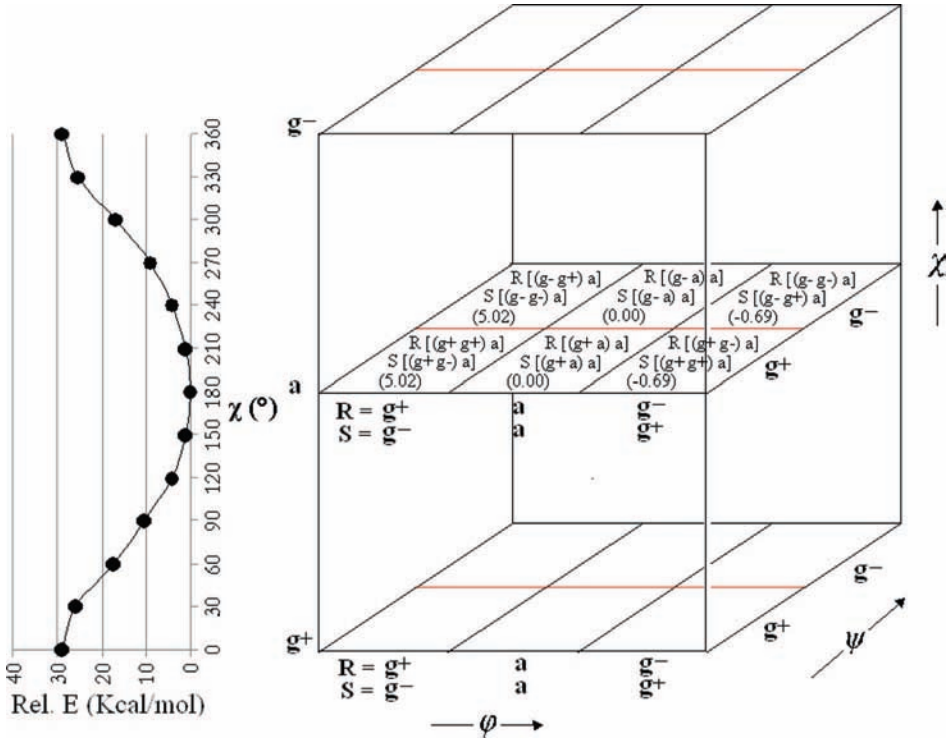


**Figure 7.** Topological pattern of the conformers of model 2, N-protonated-$\beta$-hydroxy-$\beta$-phenyl-ethylamine, enantiomers to be geometry optimized at the B3LYP/6-31G(d,p) and G3MP2B3 levels of theory.

given in kilocalories per mole, while entropy ($S$) was given in cal (mol K)$^{-1}$ units.

**3.6. Topological AIM Analysis of Electron Density.** From the geometry-optimized structures, potential hydrogen bonds (H bonds) and other intramolecular interactions were identified based on the bond distance between hydrogen and possible electron donor: oxygen. Interatomic distances were indicative of strength of the potential hydrogen bonds.[27] Hydrogen-bond angles play an important role in determining interaction strength, allowing for molecular orbital alignment. In this work, Bader's atoms in molecules (AIM) method,[29,30] employing the AIM2000 program package, was used.[30] AIM results provide exact mathematical characterization of all bonds (including H bonds) via localization of the critical points of the electron density.

**3.7. Extent of Aromaticity.** The geometries and analytical frequencies were computed at the G3MP2B3 level of theory using the Gaussian03 program. The thermodynamic enthalpy values ($H$) were calculated at 298.14 K. The aromaticity percentages were characterized by a common and universal linear scale based on the enthalpy of hydrogenation (see $\Delta H_{H2}$

**TABLE 3: Dihedral Angles, Ψ, $\varphi$, and $\chi$, Total and Relative Energies of Model 2, N-Protonated-$\beta$-hydroxy-$\beta$-phenyl-ethylamine, Computed at the B3LYP/6-31G(d,p) and G3MP2B3 Levels of Theory**

| | G3MP2B3 and [B3LYP/6-31G(d,p)] | | | | | | | | | |
|---|---|---|---|---|---|---|---|---|---|---|
| parameters | Ψ (deg) | | $\varphi$ (deg) | | $\chi$ (deg) | | energy (Hartree) | | Δ*E* (kcal/mol) | |
| *R* [(g+ g+) a] | 78.48 | [79.55] | 53.85 | [53.62] | 178.54 | [178.0] | −441.803077 | [−441.829256] | 5.05 | [5.02] |
| *R* [(g− g+) a] | −99.32 | [−98.01] | 53.81 | [53.76] | 178.37 | [177.9] | −441.803076 | [−441.829256] | 5.05 | [5.02] |
| *R* [(g+ a) a] | 74.53 | [74.35] | −168.5 | [−167.86] | −173.98 | [−173.04] | −441.811125 | [−441.837251] | 0.00 | [0.00] |
| *R* [(g− a) a] | −104.88 | [−104.28] | −168.39 | [−167.87] | −173.34 | [−173.8] | −441.811126 | [−441.837256] | 0.00 | [0.00] |
| *R* [(g+ g−) a] | 94.01 | [94.3] | −68.68 | [−68.53] | 179.63 | [179.23] | −441.812111 | [−441.838351] | −0.62 | [−0.69] |
| *R* [(g− g−) a] | −83.65 | [−83.41] | −68.32 | [−68.61] | 179.62 | [179.21] | −441.812111 | [−441.838351] | −0.62 | [−0.69] |
| *S* [(g+ g+) a] | 83.6 | [83.42] | 68.49 | [68.64] | −179.56 | [−179.18] | −441.812112 | [−441.838351] | −0.62 | [−0.69] |
| *S* [(g- g+) a] | −94.1 | [−94.36] | 68.37 | [68.68] | −179.46 | [−179.18] | −441.812111 | [−441.838351] | −0.62 | [−0.69] |
| *S* [(g+ a) a] | 105.55 | [105.01] | 168.23 | [168.1] | 172.1 | [172.77] | −441.811122 | [−441.837249] | 0.00 | [0.00] |
| *S* [(g− a) a] | −73.72 | [−74.64] | 168.07 | [168.0] | 171.98 | [173.14] | −441.811119 | [−441.837251] | 0.00 | [0.00] |
| *S* [(g+ g−) a] | 99.15 | [98.23] | −53.88 | [−53.19] | −178.22 | [−177.88] | −441.803076 | [−441.829254] | 5.05 | [5.02] |
| *S* [(g− g−) a] | −78.45 | [−79.62] | −53.93 | [−53.68] | −178.58 | [−177.77] | −441.803077 | [−441.829256] | 5.05 | [5.02] |

and $\Delta\Delta H_{H2}$ in eqs 1, 2, and 3) when cyclobutadiene and benzene were considered as −100% and +100%, respectively (Figure 3). This methodology corrects the hydrogenation reaction of the examined compound ($\Delta H_{H2}$[I]) with that of a properly chosen reference reaction ($\Delta H_{H2}$[II]), where an unsaturated analogue that does not possess any aromatic or antiaromatic character was hydrogenated (eq 2). Finally, the aromaticity value was calculated by a liner equation (eq 4)

$$\Delta H_{H2}[I] = H[1] - \{H[2] + H(H_2)\} \quad (1)$$

$$\Delta H_{H2}[II] = H[3] - \{H[4] + H(H_2)\} \quad (2)$$

$$\Delta\Delta H_{H2} = \Delta H_{H2}[I] - \Delta H_{H2}[II] \quad (3)$$

$$\text{aromaticity } \% = m\Delta\Delta H_{H2} + b \quad (4)$$

where $m = 0.7345$ and $b = -3.7474$ at the G3MP2B3 level of theory.[31]

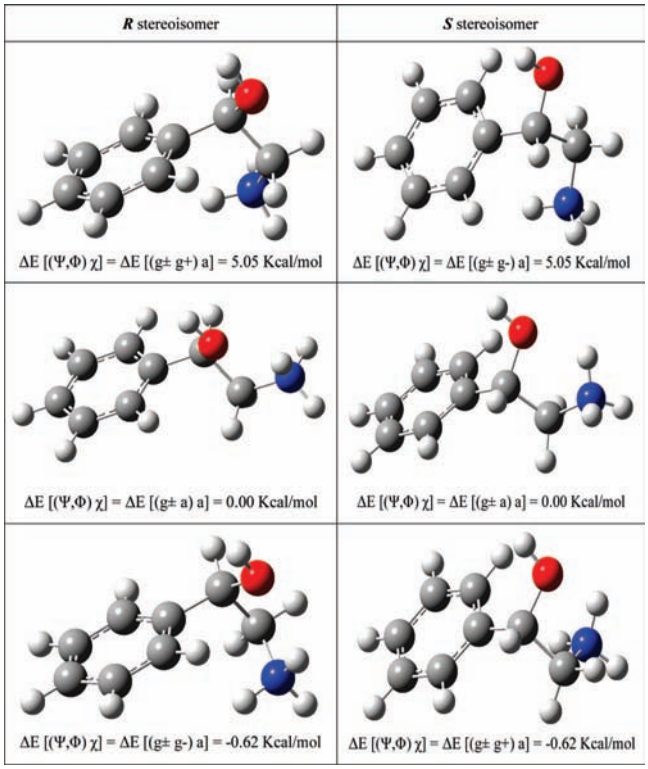


**Figure 8.** All conformations of the *R* and *S* configurations of Model 2, N-protonated-$\beta$-hydroxy-$\beta$-phenyl-ethylamine, computed at the G3MP2B3 level of theory with corresponding relative energy values. (Note that each row has a pair of enantiomers that are equal in energy.)

## 4. Results and Discussion

**4.1. Molecular Conformation and Energetics of Model 1.** It is generally assumed that by replacing a C−OH functionality with a C−F moiety one obtains a relatively good model retaining a polarized bond but eliminating a torsional mode of motion. The present paper re-examines the reliability of such an assumption.

In the case of model 1, N-protonated-$\beta$-fluoro-$\beta$-phenyl-ethylamine, in accordance with Figure 2, only two dihedral angles, $\varphi$ and Ψ, need to be considered for assessing the free conformational space. One of them is the rotation about the aromatic ring and the first carbon of the side chain [Ar−CHF], denoted as Ψ, and other is in between the α and $\beta$a carbon atoms of the side chain [ArCHF−$CH_2NH_3^{(+)}$], denoted as $\varphi$. As may be expected, this leads to a $2 \times 3 = 6$ minima potential-energy surface as illustrated in Figure 4. The optimized geometries and computed total and relative molecular energies are listed in Table 1. The six conformers show double degeneracy for both the *R* and *S* enantiomers computed at two levels of theory. The shape of all the conformers, including the highest and lowest energy conformers for the *R* and *S* isomers, is depicted in Figure 5.

The thermodynamic functions for the conformers of the *R* and *S* stereoisomers computed at two levels of theory are summarized in the Supporting Information, Table S1. Their relative values are given in Table 2.

The topological patterns for the Gibbs free energy, $\Delta G = f(\Psi,\varphi)$, and entropy, $\Delta S = f(\Psi,\varphi)$, surfaces are depicted in Figure 6.

**4.2. Molecular Conformation and Energetics of Model 2.** In the case of Model 2, N-protonated-$\beta$-hydroxy-$\beta$-phenyl-ethylamine, in accordance with Figure 2, three dihedral angles, Ψ, $\varphi$, and $\chi$, need to be considered. Two torsional modes, Ψ and $\varphi$, are related to the shape of the hydrocarbon backbone, while $\chi$ specifies the orientation of the hydroxy side chain. As it may be seen from Figure 7, the rotation about the C−OH bond, $\chi$, yields a single minimum only, corresponding to an anti orientation. In this way, the anticipated potential-energy hypersurface (PEHS) is simplified to a potential-energy surface (PES) as demonstrated by Figure 7. This PES, like the one obtained for the fluoro congener (Figure 4), again shows $2 \times 3 = 6$ minima.

The geometrical and energetic parameters, optimized at the B3LYP/6-31G(d,p) and G3MP2B3 levels of theory, are listed in Table 3. The six conformers exhibit double degeneracy again due to the equivalent gauche$^+$ and gauche$^-$ orientation of the benzene ring with respect to Ψ, the saturated chain. The molecular structures of the highest and lowest energy conformers for the *R* and *S* enantiomers are shown in Figure 8.

**TABLE 4: Thermodynamic Functional Changes of Energy ($\Delta U$), Enthalpy ($\Delta H$), Gibbs Free Energy ($\Delta G$), and Entropy ($\Delta S$) of Model 2, N-Protonated-$\beta$-hydroxy-$\beta$-phenyl-ethylamine, Computed at the B3LYP/6-31G(d,p) and G3MP2B3 Levels of Theory**

| | G3MP2B3 and [B3LYP/6-31G(d,p)] | | | | | | | |
|---|---|---|---|---|---|---|---|---|
| parameters | $\Delta U$ (kcal/mol) | | $\Delta H$ (kcal/mol) | | $\Delta G$ (kcal/mol) | | $\Delta S$ (cal/mol·K) | |
| *R* [(g+ g+) a] | 4.94 | [4.92] | 4.94 | [4.91] | 4.79 | [4.78] | 0.51 | [0.46] |
| *R* [(g− g+) a] | 4.95 | [4.92] | 4.95 | [4.92] | 4.79 | [4.78] | 0.51 | [0.45] |
| *R* [(g+ a) a] | 0.00 | [0.00] | 0.00 | [0.00] | 0.00 | [0.00] | 0.00 | [0.00] |
| *R* [(g− a) a] | 0.00 | [0.01] | 0.00 | [0.01] | −0.01 | [0.03] | 0.02 | [−0.07] |
| *R* [(g+ g−) a] | −0.53 | [−0.57] | −0.53 | [−0.57] | −0.24 | [−0.25] | −0.98 | [−1.09] |
| *R* [(g− g−) a] | −0.53 | [−0.57] | −0.53 | [−0.57] | −0.24 | [−0.24] | −0.96 | [−1.09] |
| *S* [(g+ g+) a] | −0.53 | [−0.57] | −0.53 | [−0.57] | −0.25 | [−0.24] | −0.96 | [−1.09] |
| *S* [(g− g+) a] | −0.53 | [−0.57] | −0.53 | [−0.57] | −0.25 | [−0.24] | −0.95 | [−1.11] |
| *S* [(g+ a) a] | −0.01 | [0.00] | −0.01 | [0.00] | −0.05 | [0.00] | 0.14 | [0.01] |
| *S* [(g− a) a] | −0.01 | [0.01] | −0.01 | [0.01] | −0.06 | [0.02] | 0.15 | [−0.02] |
| *S* [(g+ g−) a] | 4.94 | [4.92] | 4.94 | [4.92] | 4.79 | [4.77] | 0.51 | [0.49] |
| *S* [(g− g−) a] | 4.94 | [4.92] | 4.94 | [4.92] | 4.79 | [4.78] | 0.51 | [0.46] |

**TABLE 5: Correlation between the Relative Conformational Energy and the Shortest F···H−N Distance of Model 1 and Shortest O···H−N Distance of Model 2[a]**

| | model 1 | | model 2 | |
|---|---|---|---|---|
| parameters | $\Delta G$ (kcal/mol) | shortest F···H−N distance (Å) | $\Delta G$ (kcal/mol) | shortest O···H−N distance (Å) |
| *R* [g± g+] | 3.42 | 3.827 | 4.80 | 3.845 |
| *R* [g± a] | 0.00 | 2.042 | 0.00 | 1.951 |
| *R* [g± g−] | −1.18 | 2.265 | −0.23 | 2.133 |
| *S* [g± g+] | −1.18 | 2.276 | −0.24 | 2.129 |
| *S* [g± a] | 0.00 | 2.04 | −0.05 | 1.956 |
| *S* [g± g−] | 3.42 | 3.829 | 4.80 | 3.844 |

[a] The thermodynamic functional change of Gibbs free energy, $\Delta G$, values are computed at the G3MP2B3 level of theory.

For the various conformers of the *R* and *S* enantiomers, the thermodynamic functions obtained at two levels of theory are listed in the Supporting Information, Table S2. The corresponding relative values ($\Delta U$, $\Delta H$, $\Delta G$, and $\Delta S$) are summarized in Table 4.

The topological patterns for the Gibbs free energy, $\Delta G = f(\Psi,\varphi)$, and entropy, $\Delta S = f(\Psi,\varphi)$, surfaces are shown in Figure 9.

**4.3. Intramolecular Hydrogen Bonding.** It may well be anticipated that, in intramolecular hydrogen bonds, the $-NH_3^{(+)}$ moiety will be the proton donor. Also, the most obvious proton acceptor may be the heteroatom, fluorine in model 1 and oxygen in model 2. The shortest distances are listed in the right-hand side column in Table 5. The first and last entries in each of the tables are too long excluding the possibility of hydrogen bonds. The central columns in these tables list the relative stabilities on the $\Delta G$ scales. Clearly, the most stable structures do not exhibit the shortest distances. This observation suggests that hydrogen bonding is not the most influential stabilizing factor in determining the overall stability of the various conformations.

AIM analysis revealed (Figure 10) that, in addition to regular hydrogen bonds, such as F···H−N and HO···H−N, there is another noncovalent interaction between the aromatic $\pi$-electron system of the benzene ring and the positively charged N−H moiety (Ar···H−N). Such cationic interactions with thr $\pi$-electron system may be assumed to occur as a special type of hydrogen bond. This occurs when $\psi$ assumes a g+ conformation as shown in Figure 10. The parameters of the AIM analysis, such as the density of the bond critical point, $\rho_b$, and Laplacian of $\rho_b$, denoted as $\nabla^2\rho_b$, are listed in Tables 6 and 7. Finally, it

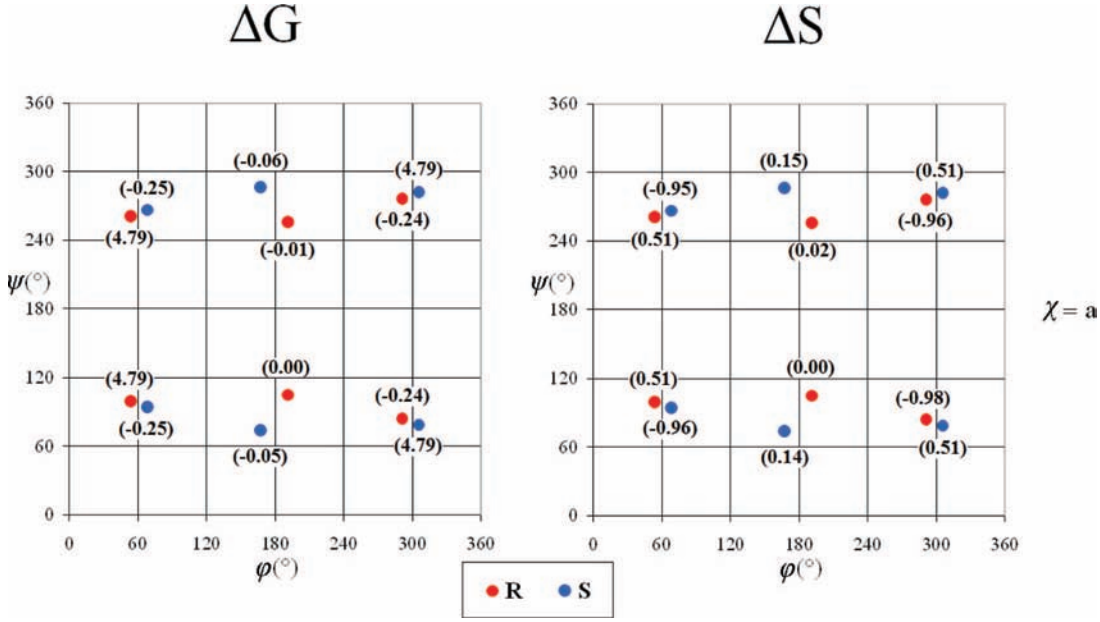


**Figure 9.** Topological representation of the optimized geometries of Model 2, N-protonated-$\beta$-hydroxy-$\beta$-phenyl-ethylamine, dihedral angles $\Psi$ and $\varphi$ corresponding to the vertical and horizontal axes, respectively. Relative energies are given in units of kcal/mol and calculated at the G3MP2B3 level of theory.

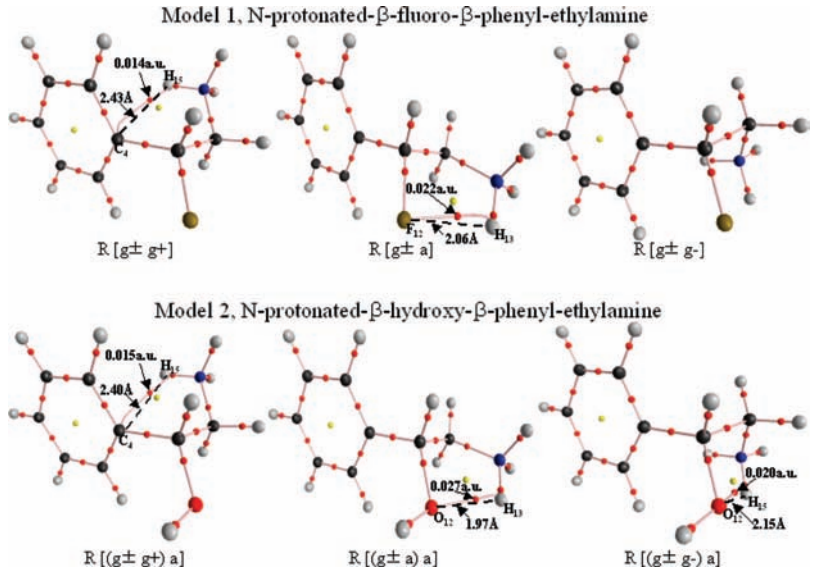


**Figure 10.** *R* conformers of models 1 and 2. All of the hydrogen bonds, which were determined by the program AIM, are shown together with their distance and $\rho_b$ charge density value at the G3MP2B3 level of theory.

**TABLE 6: Electron Densities, $\rho_b$ (au), and Laplacian of Electron Densities, $\nabla^2\rho_b$ (au), of Bond Critical Points of All Conformers of Model 1, N-Protonated-*β*-fluoro-*β*-phenyl-thylamine, at the G3MP2B3 Level of Theory**

| | N−H···C−C | | | N−H···F−C | | |
|---|---|---|---|---|---|---|
| parameters | $\rho_b$ (au) | $\nabla^2\rho_b$ (au) | bond length (Å) | $\rho_b$ (au) | $\nabla^2\rho_b$ (au) | bond length (Å) |
| *R* [g± g+] | 0.0142 | −0.012 | 2.4285 | | | |
| *R* [g± a] | | | | 0.0215 | −0.024 | 2.0605 |
| *R* [g± g−] | | | | | | |
| *S* [g± g+] | | | | | | |
| *S* [g± a] | | | | 0.0215 | −0.024 | 2.0602 |
| *S* [g± g−] | 0.0143 | −0.012 | 2.4246 | | | |

**TABLE 7: Electron Densities, $\rho_b$ (au), and Laplacian of Electron Densities, $\nabla^2\rho_b$ (au), of Bond Critical Points of All Conformers of Model 2, N-Protonated-*β*-hydroxy-*β*-phenyl-ethylamine, at the G3MP2B3 Level of Theory**

| | N−H···C−C | | | N−H···O−C | | |
|---|---|---|---|---|---|---|
| parameters | $\rho_b$ | $\nabla^2\rho_b$ | bond length (Å) | $\rho_b$ | $\nabla^2\rho_b$ | bond length (Å) |
| *R* [(g± g+) a] | 0.0145 | −0.013 | 2.397 | | | |
| *R* [(g± a) a] | | | | 0.0271 | −0.026 | 1.965 |
| *R* [(g± g−) a] | | | | 0.0199 | −0.021 | 2.1484 |
| *S* [(g± g+) a] | | | | 0.0199 | −0.021 | 2.1495 |
| *S* [(g± a) a] | | | | 0.0271 | −0.026 | 1.9662 |
| *S* [(g± g−) a] | 0.0144 | −0.013 | 2.3981 | | | |

**TABLE 8: $\Delta H_{H2}$[I], $\Delta H_{H2}$[I], and Aromaticity Values for Model 1, N-Protonated-*β*-fluoro-*β*-phenyl-ethylamine**

| parameters | $\Delta H_{H2}$[I] (kJ mol$^{-1}$) | $\Delta H_{H2}$[II] (kJ mol$^{-1}$) | $\Delta\Delta H_{H2}$ (kJ mol$^{-1}$) | aromaticity (%) |
|---|---|---|---|---|
| *R* [g± g+] | +36.32 | −110.80 | 147.12 | 104.3 |
| *R* [g± a] | +38.20 | −110.80 | 149.00 | 105.7 |
| *R* [g± g−] | +30.83 | −110.80 | 141.63 | 100.3 |
| *S* [g± g+] | +35.55 | −110.80 | 146.35 | 103.7 |
| *S* [g± a] | +33.67 | −110.80 | 144.47 | 102.4 |
| iS [g± g−] | +30.93 | −110.80 | 141.73 | 100.4 |

should be noted that there is no F···H−N hydrogen bond in the g− conformer of model 1.

**4.4. Extent of Aromaticity in Varying Conformations.** Aromaticity measures the tightness of $\pi$ electrons bound to the atomic nuclei. By convention, benzene is taken to be of 100% aromaticity.[29] If the molecule has a positive charge, it has one fewer electron than positive nuclear charge. Thus, the fewer electrons are bound more tightly to the nuclei of the ring. Since both of the models studied have a protonated amine, $-NH_3^{(+)}$, therefore due to the positive charge within the molecule, a slight elevation in the aromaticity percentage values is to be expected. These percentage values could vary with conformation as the conformations may have noticeable intramolecular interactions. The computed numerical values are summarized in Tables 8 and 9.

**TABLE 9: $\Delta H_{H2}$[I], $\Delta H_{H2}$[I], and Aromaticity Values for Model 2, N-Protonated-*β*-hydroxy-*β*-phenyl-ethylamine**

| parameters | $\Delta H_{H2}$[I] (kJ mol$^{-1}$) | $\Delta H_{H2}$[II] (kJ mol$^{-1}$) | $\Delta\Delta H_{H2}$ (kJ mol$^{-1}$) | aromaticity (%) |
|---|---|---|---|---|
| *R* [(g± g+) a] | 38.24 | 110.80 | 149.04 | 105.7 |
| *R* [(g± a) a] | 38.68 | −110.80 | 149.48 | 106.0 |
| *R* [(g± g−) a] | 31.94 | −110.80 | 142.74 | 101.1 |
| *S* [(g± g+) a] | 36.66 | −110.80 | 147.46 | 104.6 |
| *S* [(g± a) a] | 35.24 | −110.80 | 146.04 | 103.5 |
| *S* [(g± g−) a] | 32.03 | −110.80 | 142.83 | 101.2 |

In viewing the foregoing, the fluorine analogue (model 1) gives a particular pattern where the weak or no hydrogen bond, involving H−O···H−N or F···H−N, has smaller aromaticity and the strong hydrogen bond leads to higher aromaticity percentage. The charge and aromatic interaction were very similar to each other, both in terms of aromaticity percentage and in $\rho_b$.

**4.5. Comparison between Model 1 and Model 2.** At first glance, there is no remarkable difference between models 1 and 2 on the basis of their IR spectra (Supporting Information, Figure S1). However, the difference of the two spectra (Figure 11) shows significant differences between the two vibrational systems not only at the high end of the spectrum (over 3000 cm$^{-1}$), where the O−H stretch is present in model 2, but also at the low end of the spectrum (less than 1500 cm$^{-1}$) as well.

The other difference between the two models, as noted earlier, is the nonequivalence of the proton-accepting ability between the lone pairs of fluorine and those of oxygen. Presumably, the fluorine lone pairs are more tightly bound and polarizable to a smaller extent upon approach of a protic hydrogen.

The difference of aromaticity values between the phenyl group of models 1 and 2 is very small ranging from 0.3% and

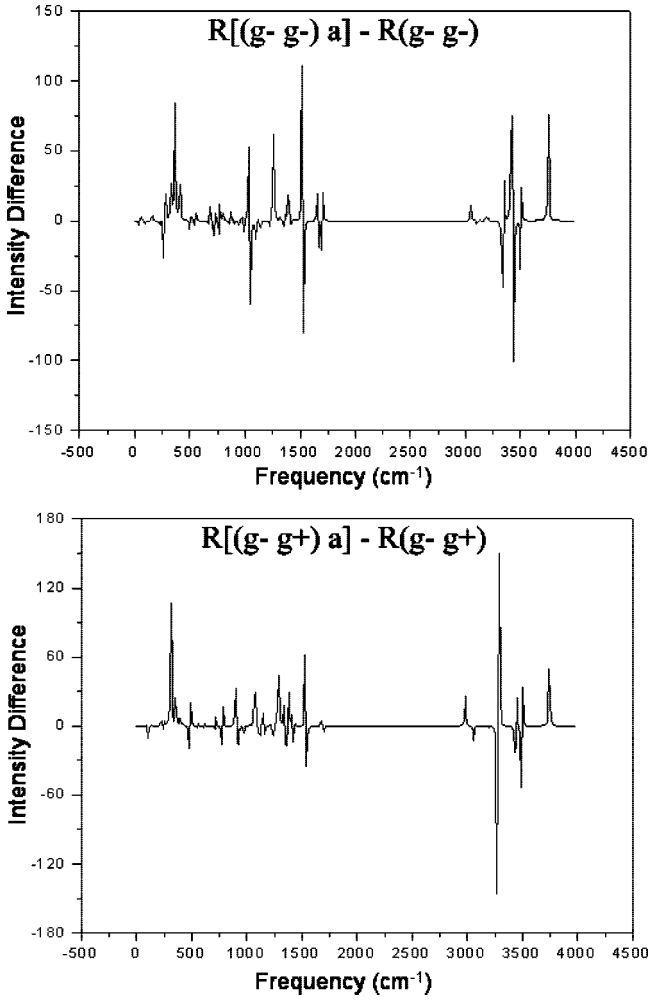


**Figure 11.** Difference IR spectra of selected conformers of models 1 and 2 computed at the G3MP2B3 level of theory.

1.4%. The aromaticity percentage for the fluoro and hydroxy congeners was 105.7% and 106.0%, respectively, in the case for the strong intramolecular hydrogen bond of F···H−N and H−O···H−N types in the a conformations. For the weak or no hydrogen bond in the g− conformation, the aromaticity percentage for the fluoro and hydroxy congeners was observed to be 100.3% and 101.1%, respectively. The aromatic−cation interaction in the g+ conformations for fluoro and hydroxy congeners showed a small but noticeable difference, being 104.3% and 105.7%, respectively.

In contrast to any small differences listed above, the geometries of the various conformations of models 1 and 2 are rather close to each other.

## 5. Conclusions

N-Protonated-$\beta$-fluoro-$\beta$-phenyl-ethylamine (model 1) and N-protonated-$\beta$-hydroxy-$\beta$-phenyl-ethylamine model (model 2) were used to mimic noradrenaline closely and at some distance adrenaline. Replacement of the −OH functionality in model 2 by −F to generate a simpler model with fewer dihedral angles to be varied led to a prototype system (model 1). Such a simpler mimic was quite useful in determining molecular structures. However, the vibrational pattern is slightly modified as model 2 has three fewer normal modes of motion due to the absence of a hydrogen atom. This is revealed by the IR difference spectra. Also, while weak hydrogen bonds of the type H−O···H−N interactions still exist in model 2, such F···H−N interactions, do not emerge in model 1.

In contrast to the foregoing, the changing pattern of the extent of aromaticity, due to intramolecular interaction, varies within 0.3% and 1.4% between models 1 and 2. The aromatic−cation interaction yielded very similar aromatic percentage values for the fluoro and hydroxy congeners.

**Acknowledgment.** D.J.R.L. and N.J.G. thank Professor Suzanne Stevenson, Vice-Dean of the Faculty of Arts and Science at the University of Toronto, for support within the Research Opportunity Program associated with their participation at the 2008 Summer Workshop held at the University of Szeged. The continuous support of the Global Institute of Computational Molecular and Materials Science (www.giocomms.org) and Drug Discovery Research Center (www.drugcent.com) are gratefully acknowledged. The authors also thank Professor Arpad Kucsman and Dr. Sinisa Vukovic for helpful suggestions.

**Supporting Information Available:** This material is available free of charge via the Internet at http://pubs.acs.org.

## References and Notes

(1) Bates, W. H. The therapeutic properties of the suprarenal capsule. *J. Am. Med. Assoc.* **1900**, *35*, 346–348.

(2) Aronson, J. K. "Where name and image meet"−the argument for "adrenaline". *Br. Med. J.* **2000**, *320*, 506–509.

(3) Yamashima, T. Jokichi Takamine (1854−1922), the samurai chemist, and his work on adrenalin. *J. Med. Biogr.* **2003**, *11* (2), 95–102.

(4) Stolz, F. Ueber Adrenalin Und Alkylaminoacetobrenzcatechin. *Ber.* **1904**, *37*, 4149–4154.

(5) Liu, T.; Huang, M.; Yu, Z.; Yan, D. Theoretical study on the supramolecular complexes of 12-crown-4 with adrenaline. *THEOCHEM* **2006**, *776*, 97–104.

(6) Nagatsu, T. The catecholamine system in health and disease - Relation to tyrosine 3-monooxygenase and other catecholamine-synthesizing enzymes. *Proc. Jpn. Acad., Ser. B* **2006**, *82* (10), 388–415.

(7) Carcabal, P.; Snoek, L. C.; van Mourik, T. A computational and spectroscopic study of the gas-phase conformers of adrenaline. *Mol. Phys.* **2005**, *103* (11−12), 1633–1639.

(8) Bennett, M. R. One hundred years of adrenaline: the discovery of autoreceptors. *Clin. Auton. Res.* **1999**, *9* (3), 145–159.

(9) Gromada, J.; Bokvist, K.; Ding, W.; Barg, S.; Buschard, K.; Renstrom, E.; Rorsman, P. Adrenaline Stimulates Glucagon Secretion in Pancreatic A-Cells by Increasing the $Ca^{2+}$ Current and the Number of Granules Close to the L-Type $Ca^{2+}$ Channels. *J. Gen. Physiol.* **1997**, *110*, 217–228.

(10) Howlett, K.; Galbo, H.; Lorentsen, J.; Bergeron, R.; Zimmerman-Belsing, T.; Bulow, J.; Feldt-Rasmussen, U.; Kjaer, M. Effect of adrenaline on glucose kinetics during exercise in adrenalectomised humans. *J. Physiol.* **1999**, *519* (3), 911–921.

(11) Baltzan, M. A.; Andres, R.; Cader, G.; Zierler, K. L. Effects of Epinephrine on Forearm Blood Flow and Metabolism in Man. *J. Clin. Invest.* **1965**, *44* (1), 80–92.

(12) Song, Y.; Zhou, J.; Song, Y.; Wei, Y.; Wang, H. Density-functional theory studies on standard electrode potentials of half reaction for L-adrenaline and adrenalinequinone. *Bioorg. Med. Chem. Lett.* **2005**, *15* (21), 4671–4680.

(13) Bao, X.; Lu, C. M.; Liu, F.; Gu, Y.; Dalton, N. D.; Zhu, B.; Foster, E.; Chen, J.; Karliner, J. S.; Ross, J.; Simpson, P. C.; Ziegler, M. G. Epinephrine is required for normal cardiovascular responses to stress in the phenylethanolamine n-methyltransferase knockout mouse. *Circulation* **2007**, *116* (9), 1024–1031.

(14) Alagona, G.; Ghio, C. Competitive H-bonds in vacuo and in aqueous solution for N-protonated adrenaline and its monohydrated complexes. *THEOCHEM* **2007**, *811* (1−3), 223–240.

(15) Gasparro, D. M.; Almeida, D. R. P.; Dobo, S. M.; Torday, L. L.; Varro, A.; Papp, J. G. An ab initio and DFT conformational analysis of unsubstituted and omega-substituted ethyl-benzene: (Ph-$CH_2$-$CH_2$-Z; Z = -H, -F, -$NH_3^+$, -$CH_3$). *THEOCHEM* **2002**, *585*, 167–179.

(16) Frisch, M. J.; Trucks, G. W.; Schlegel, H. B.; Scuseria, G. E.; Robb, M. A.; Cheeseman, J. R.; Montgomery, J. A., Jr.; Vreven, T.; Kudin, K. N.; Burant, J. C.; Millam, J. M.; Iyengar, S. S.; Tomasi, J.; Barone, H.; Mennucci, B.; Cossi, M.; Scalmani, G.; Rega, N.; Petersson, G. A.; Nakatsuji, H.; Hada, M.; Ehara, M.; Toyota, K.; Fukada, R.; Hasegawa, J.;

Ishida, M.; Nakajima, T.; Honda, Y.; Kitao, O.; Nakai, H.; Klene, M.; i, X.; Knox, J. E.; Hratchian, H. P.; Cross, J. B.; Bakken, V.; Adamo, C.; Jaramillo, J.; Gomperts, R.; Stratmann, R. E.; Yazyev, O.; Austin, A. J.; Cammi, R.; Pomelli, C.; Ochterski, J. W.; Ayala, P. Y.; Morokuma, K.; Voth, G. A.; Salvador, P.; Dannenberg, J. J.; Zakrzewski, V. G.; Dapprich, S.; Daniels, A. D.; Strain, M. C.; Farkas, O.; Maliek, D. K.; Rabuck, A. D.; Raghavachari, K.; Foresman, J. B.; Ortiz, J. V.; Cui, Q.; Baboul, A. G.; Clifford, S.; Cioslowski, J.; Stefanov, B. B.; Liu, G.; Liashenko, A.; Piskorz, P.; Komaromi, I.; Martin, R. L.; Fox, D. J.; Keith, T.; Al-Laham, M. A.; Peng, C. Y.; Nanayakkara, A. ; Challacombe, M.; Gill, P. M. W.; Johnson, B.; Chen, W.; Wong, M. W.; Gonzalez, C.; Pople, J. A. *Gaussian 03*, Revision B.01; Gaussian Inc.: Wallingford, CT, 2004.

(17) Hehre, W. J.; Radom, L.; Schleyer, P. v. R.; Pople, J. A. *Ab Initio Molecular Orbital Theory*; John Wiley & Sons: New York, 1986.

(18) Roothan, C. C. New developments in molecular orbital theory. *Rev. Mod. Phys.* **1951**, *23*, 69–89.

(19) Hehre, W. J.; Ditchfie, R.; Pople, J. A. Self-Consistent Molecular-Orbital Methods. 12. Further Extensions of Gaussian-Type Basis Sets for Use in Molecular-Orbital Studies of Organic-Molecules. *J. Chem. Phys.* **1972**, *56* (5), 2257.

(20) Ditchfie, R.; Hehre, W. J.; Pople, J. A. Self-Consistent Molecular-Orbital Methods. 9. Extended Gaussian-Type Basis for Molecular-Orbital Studies of Organic Molecules. *J. Chem. Phys.* **1971**, *54* (2), 724.

(21) Hariharan, P. C.; Pople, J. A. Influence of Polarization Functions on Molecular-Orbital Hydrogenation Energies. *Theor. Chim. Acta* **1973**, *28* (3), 213–222.

(22) Becke, A. D. Density-functional thermochemistry. 4. A new dynamical correlation functional and implications for exact-exchange mixing. *J. Chem. Phys.* **1996**, *104* (3), 1040–1046.

(23) Lee, C. T.; Yang, W. T.; Parr, R. G. Development of the Colle-Salvetti Correlation-Energy Formula into A Functional of the Electron-Density. *Phys. Rev. B* **1988**, *37* (2), 785–789.

(24) Curtiss, L. A.; Redfern, P. C.; Raghavachari, K.; Rassolov, V.; Pople, J. A. Gaussian-3 theory using reduced Moller-Plesset order. *J. Chem. Phys.* **1999**, *110* (10), 4703–4709.

(25) Curtiss, L. A.; Raghavachari, K.; Redfern, P. C.; Rassolov, V.; Pople, J. A. Gaussian-3 (G3) theory for molecules containing first and second-row atoms. *J. Chem. Phys.* **1998**, *109* (18), 7764–7776.

(26) Baboul, A. G.; Curtiss, L. A.; Redfern, P. C.; Raghavachari, K. Gaussian-3 theory using density functional geometries and zero-point energies. *J. Chem. Phys.* **1999**, *110* (16), 7650–7657.

(27) Tang, T.-H.; Deretey, E.; Knak Jensen, S. J.; Csizmadia, I. G. Hydrogen bonds: Relation between lengths and electron densities at bond critical points. *Eur. Phys. J. D* **2006**, *37*, 217–222.

(28) Bader, R. F. W. Atoms in Molecules. *Acc. Chem. Res.* **1985**, *18*, 9–15.

(29) Bader, R. F. W. A Quantum Theory of Molecular Structure and Its Applications. *Chem. Rev.* **1991**, *91*, 893.

(30) Biegler-König, F.; Schönbohm, J.; Bayles, D. AIM2000-Programm to Analyze and Visualize Atoms in Molecules. *J. Comput. Chem.* **2001**, *22*, 545–559.

(31) Mucsi, Z.; Viskolcz, B.; Csizmadia, I. G. A Quantitaive Scale for the Degree of Aromaticity and Anti-aromaticity: A Comparison of Theoretical and Experimental Enthalpies of Hydrogenation. *J. Phys. Chem. A* **2007**, *111*, 1123–1132.

JP807353N